

On the theory of galvanomagnetic transport properties of continuous double- and multiple-layer metallic thin films

This article has been downloaded from IOPscience. Please scroll down to see the full text article.

1989 J. Phys.: Condens. Matter 1 3919

(<http://iopscience.iop.org/0953-8984/1/25/004>)

View [the table of contents for this issue](#), or go to the [journal homepage](#) for more

Download details:

IP Address: 171.66.16.93

The article was downloaded on 10/05/2010 at 18:20

Please note that [terms and conditions apply](#).

On the theory of galvanomagnetic transport properties of continuous double- and multiple-layer metallic thin films

Chu-Xing Chen†

224 East 4th Street, Tucson, AZ 85705, USA

Received 17 March 1988, in final form 22 September 1988

Abstract. Theoretical solutions have been derived for the galvanomagnetic transport properties of double- and multiple-layer continuous metallic thin films. Interface scattering as well as external surface scattering of conduction electrons have been taken into account when solving for the electron distribution function in the presence of a transverse magnetic field. The electrical conductivities and the Hall coefficients of thin films are also given.

1. Introduction

The galvanomagnetic transport properties of metallic thin films have been studied both theoretically and experimentally [1–9] with great interest. The first analysis of the conductivity of metallic thin films in the presence of transverse magnetic field was done by Sondheimer [1], who extended Fuchs' theory of thin-film electrical conductivity [10, 11] to the existence of a transverse magnetic field. Later Sondheimer's theory was applied extensively to studies of single-layer thin films, and some other approaches have been proposed [7–9]. In recent years, new thin-film growth technologies such as sputtering and molecular beam epitaxy have been used to develop new types of thin film such as double- and multiple-layer films, which in turn have attracted attention to their interesting behaviours [12–20]. When two metallic crystals grow on top of each other, the overall physical properties carry part of the coherence or incoherence between the two. The physical mechanisms of metal–metal interface structures and their properties have been studied theoretically [21–25], and primary results reveal that electron density appears to have somewhat special states at the interface like that of the surfaces. To give an exact solution to the electron–interface scattering process is very difficult, however. In practical situations, the interface roughness, just as its counterpart at the external surface, involves many hard-to-control elements, making exact modelling extremely difficult. The use of average scattering parameters over the entire film for interfaces (and for external surfaces) becomes not only necessary and useful in understanding the interface-related physics, but also provides the first realistic approach to the problem. These types of scattering parameters, first introduced by Fuchs in 1938 [10], have been used extensively in research into thin film transport phenomena in both theory and experiment, and have been quite successful over the years. As for metallic double- and

† Send correspondence to: Department of Physics, University of Arizona, Tucson, AZ 85721, USA

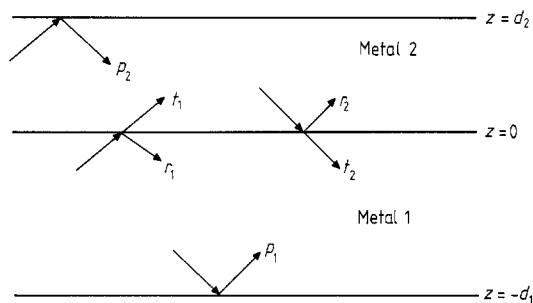


Figure 1. A schematic illustration of the double-layer thin films.

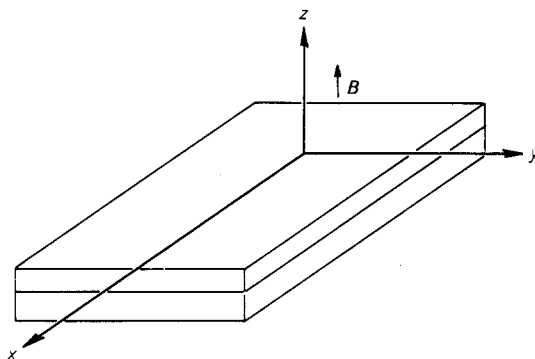


Figure 2. Illustration of coordinate system.

multiple-layer films, several theories have been proposed [12–15, 18–20] to interpret the electrical conductivities in the absence of magnetic field.

In this paper we shall derive general solutions for the Boltzmann transport equation of conduction electrons for double- and multiple-layer metallic thin films in the presence of a transverse magnetic field. The results are presented in terms of surface and interface scattering parameters. Finally we give the solutions to the electrical conductivity and the Hall coefficient.

2. Double-layer thin films

2.1. Electron distribution functions

Consider a double-layer thin film with layer thicknesses d_1 and d_2 respectively, as shown in figure 1. The surface reflection coefficients p_1 and p_2 represent the amount of electrons that are specularly reflected by the surfaces. The interface contributions to the transport phenomena are represented by the transmission coefficients t_1 and t_2 , which stand for the specularly transmitted part of the electrons, and the reflection coefficients r_1 and r_2 , which stand for the specularly reflected part of the electrons. The film is placed in an x - y plane and the magnetic field is along the z axis, as shown in figure 2. We assume that the bulk values of the electrical conductivities σ_1 and σ_2 , and the mean free paths λ_1 and λ_2 are known, or can be determined otherwise. We also assume that the diffusion

scattered electrons have the same possibilities of going in any direction, i.e., 4π solid angle in the case of interfaces and 2π in the case of surfaces.

The electron distribution function can be written as

$$f(v, z) = f_0 + f_{1,2}(v, z) \tag{1}$$

where f_0 is the Fermi distribution function, and $f_1(v, z)$ and $f_2(v, z)$ are the deviations from f_0 in metals 1 and 2, respectively. The Boltzmann transport equation has the form

$$\frac{\partial f_{1,2}}{\partial z} + \frac{f_{1,2}}{\tau_{1,2}v_z} - \frac{eB}{mv_z} \left(v_y \frac{\partial f_{1,2}}{\partial v_x} - v_x \frac{\partial f_{1,2}}{\partial v_y} \right) = \frac{e}{mv_z} \left(E_x \frac{\partial f_0}{\partial v_x} + E_y \frac{\partial f_0}{\partial v_y} \right). \tag{2}$$

Applying Sondheimer's method, we define

$$f_1 = (v_x c_{11} + v_y c_{12}) \partial f_0 / \partial v \tag{3}$$

$$f_2 = (v_x c_{21} + v_y c_{22}) \partial f_0 / \partial v \tag{4}$$

$$g_1 = c_{11} - ic_{12} \tag{5}$$

$$g_2 = c_{21} - ic_{22} \tag{6}$$

and

$$E^* = E_x - iE_y. \tag{7}$$

Now we have a new form of equation (2):

$$\frac{\partial g_{1,2}}{\partial z} + \frac{g_{1,2}}{\tau_{1,2}v_z} + i \frac{eB}{mv_z} g_{1,2} = \frac{e}{mvv_z} E^*. \tag{8}$$

This can be further reduced to

$$\frac{\partial g_{1,2}}{\partial z} + \frac{g_{1,2}}{\tau_{1,2}^*v_z} = \frac{e}{mvv_z} E^* \tag{9}$$

where

$$\tau_{1,2}^* = 1/(1/\tau_{1,2} + i\alpha) \tag{10}$$

and

$$\alpha = eB/m. \tag{11}$$

The general solutions to (9) are

$$g_1^+(\bar{v}, z) = \frac{e\tau_1^* E^*}{mv} \left[1 + F_1^+(\bar{v}) \exp\left(-\frac{z+d_1}{\tau_1^*v_z}\right) \right] \quad v_z > 0, -d_1 < z < 0 \tag{12}$$

$$g_1^-(\bar{v}, z) = \frac{e\tau_1^* E^*}{mv} \left[1 + F_1^-(\bar{v}) \exp\left(-\frac{z}{\tau_1^*v_z}\right) \right] \quad v_z < 0, -d_1 < z < 0 \tag{13}$$

$$g_2^+(\bar{v}, z) = \frac{e\tau_2^* E^*}{mv} \left[1 + F_2^+(\bar{v}) \exp\left(-\frac{z}{\tau_2^*v_z}\right) \right] \quad v_z > 0, 0 < z < d_2 \tag{14}$$

$$g_2^-(\bar{v}, z) = \frac{e\tau_2^* E^*}{mv} \left[1 + F_2^-(\bar{v}) \exp\left(-\frac{z-d_2}{\tau_2^*v_z}\right) \right] \quad v_z < 0, 0 < z < d_2. \tag{15}$$

The boundary conditions can be derived as

$$g_1^+(v_z, z = -d_1) = p_1 g_1^-(v_z, z = -d_1) \quad (16)$$

$$g_1^-(v_z, z = 0) = r_1 g_1^+(-v_z, z = 0) + t_2 g_2^-(v_z, z = 0) \quad (17)$$

$$g_2^+(v_z, z = 0) = r_2 g_2^+(-v_z, z = 0) + t_1 g_1^+(v_z, z = 0) \quad (18)$$

$$g_2^-(v_z, z = d_2) = p_2 g_2^+(-v_z, z = d_2). \quad (19)$$

Combining (12)–(15) with (16)–(19), we obtain a set of four linear equations for F . The exact solutions are complicated and are given in the Appendix; here we only give solutions under the approximation of small r and t , which represent relatively rough interfaces.

$$F_1^+ = -1 + p_1 - p_1 \exp(-d_1/\tau_1 v_z) \quad (20)$$

$$F_1^- = -1 + r_1 + t_2(\tau_2/\tau_1) - r_1 \exp(-d_1/\tau_1 v_z) - t_2(\tau_2/\tau_1) \exp(-d_2/\tau_2 v_z) \quad (21)$$

$$F_2^+ = -1 + r_2 + t_1(\tau_1/\tau_2) - r_2 \exp(-d_2/\tau_2 v_z) - t_1(\tau_1/\tau_2) \exp(-d_1/\tau_1 v_z) \quad (22)$$

$$F_2^- = -1 + p_2 - p_2 \exp(d_2/\tau_2 v_z). \quad (23)$$

Substituting (20)–(23) into (12)–(15), we obtain all final results of conduction electron distribution functions for double-layer thin films with transverse magnetic field present.

2.2. Conductivity and the Hall coefficient

The electrical current densities inside metal 1 are

$$J_{1x} = -2e(m^3/h^3) \iiint c_{11} v_x^2 (\partial f/\partial v) dv_x dv_y dv_z \quad (24)$$

$$J_{1y} = -2e(m^3/h^3) \iiint c_{12} v_y^2 (\partial f/\partial v) dv_x dv_y dv_z. \quad (25)$$

We can write the same expressions for metal 2. Define

$$J^* = J_x - iJ_y \quad (26)$$

then

$$J_{1,2}^* = -2\pi e(m^3/h^3) \int_0^\pi d\theta \int_0^\infty g_{1,2} v^4 \sin^3 \theta (\partial f_0/\partial v) dv. \quad (27)$$

Substituting the solutions for $g_{1,2}$ into (27), we obtain the results for electrical current densities

$$J_1^* = -\frac{4\pi e^2 m^2}{h^3} E^* \int_0^\infty dv \int_1^\infty dt v^3 \frac{\partial f_0}{\partial v} \tau_1^* \left(\frac{1}{t^2} - \frac{1}{t^4} \right) \times \left[1 + (F_1^+/2) \exp\left(-\frac{z+d_1}{\tau_1^* v} t\right) + (F_1^-/2) \exp\left(\frac{z}{\tau_1^* v} t\right) \right] \quad (28)$$

$$J_2^* = -\frac{4\pi e^2 m^2}{\hbar^3} E^* \int_0^\infty dv \int_1^\infty dt v^3 \frac{\partial f_0}{\partial v} \tau_2^* \left(\frac{1}{t^2} - \frac{1}{t^4} \right) \times \left[1 + (F_2^+/2) \exp\left(-\frac{z}{\tau_2^* v} t\right) + (F_2^-/2) \exp\left(\frac{z-d_2}{\tau_2^* v} t\right) \right]. \tag{29}$$

The electrical conductivity is defined as

$$\sigma_{1,2} = \frac{\text{Re}(J_{1,2}^*)}{E_x} \Big|_{\text{Im}(J_{1,2}^*)=0} \tag{30}$$

and the Hall coefficient is defined as

$$R_{H1,2} = \frac{E_y}{B \text{Re}(J_{1,2}^*)} \Big|_{\text{Im}(J_{1,2}^*)=0}. \tag{31}$$

The electron distribution functions depend upon z . To deduce some experimentally measurable quantities, we have to average over the entire thin film. The actual average is done for each individual layer, and the film average can be easily carried out thereafter. The results are

$$\sigma_1 = \sigma_1^0 \left(1 - (3\lambda_1/4d_1) \int_1^\infty dt (1/t^3 - 1/t^5)(F_1^+ + F_1^-)[\exp(-d_1 t/\lambda_1) - 1] \right) \tag{32}$$

$$\sigma_2 = \sigma_2^0 \left(1 - (3\lambda_2/4d_2) \int_1^\infty dt (1/t^3 - 1/t^5)(F_2^+ + F_2^-)[\exp(-d_2 t/\lambda_2) - 1] \right) \tag{33}$$

$$R_{H1} = R_{H1}^0 \left(1 - (3\lambda_1/4d_1) \int_1^\infty dt (1/t^3 - 1/t^5)(F_1^+ + F_1^-) \times [\exp(-d_1 t/\lambda_1) - 1] \right)^{-1} \tag{34}$$

$$R_{H2} = R_{H2}^0 \left(1 - (3\lambda_2/4d_2) \int_1^\infty dt (1/t^3 - 1/t^5)(F_2^+ + F_2^-)[\exp(-d_2 t/\lambda_2) - 1] \right)^{-1}. \tag{35}$$

Figure 3 shows the calculated electrical conductivity calculations for metal 1. The assumed thin film has metal layers of equal thickness with various interface parameters. From top to bottom both r and t decrease, i.e., the interface roughness increases. Figure 4 shows the corresponding Hall coefficients under the same assumptions as figure 3. We notice first that when layers become very thick, both electrical conductivities and Hall coefficients approach their bulk values, as they must do for the results to make sense. In general the results agree with those for single-layer thin films [2, 8]; the main difference is the coupling effect between the two metals, as revealed in equations (21) and (22).

3. Multiple-layer thin films

3.1. Electron distribution function

Due to their strong structural coherence across each individual layer, metallic multiple-layer thin films such as superlattices are systems with enhanced interface effects. Exper-

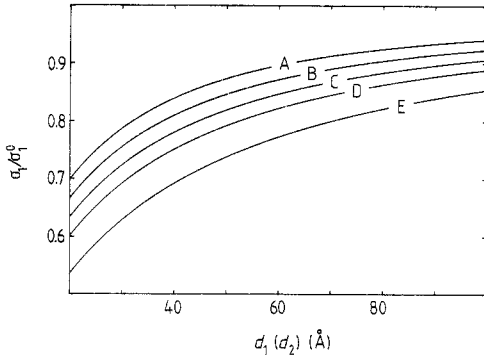


Figure 3. σ_1/σ_1^0 versus layer thickness. $\lambda_1 = 50 \text{ \AA}$, $\lambda_2 = 150 \text{ \AA}$, $p_1 = 0.1$, $p_2 = 0.2$; (A) $r_1 = t_1 = 0.25$, $r_2 = t_2 = 0.35$; (B) $r_1 = t_1 = 0.2$, $r_2 = t_2 = 0.3$; (C) $r_1 = t_1 = 0.15$, $r_2 = t_2 = 0.25$; (D) $r_1 = t_1 = 0.1$, $r_2 = t_2 = 0.2$; (E) $r_1 = r_2 = 0.3$, $t_1 = t_2 = 0$.

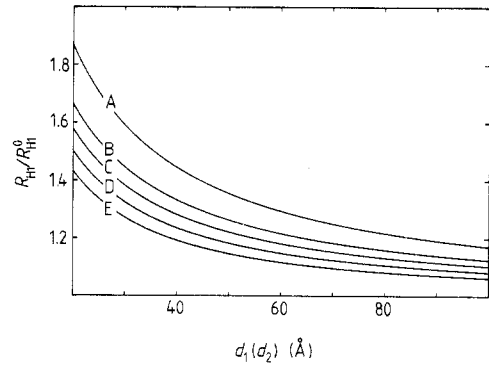


Figure 4. R_{H1}/R_{H1}^0 versus layer thickness. $\lambda_1 = 50 \text{ \AA}$, $\lambda_2 = 150 \text{ \AA}$, $p_1 = 0.1$, $p_2 = 0.2$; (A) $r_1 = r_2 = 0.3$, $t_1 = t_2 = 0$; (B) $r_1 = t_1 = 0.1$, $r_2 = t_2 = 0.2$; (C) $r_1 = t_1 = 0.15$, $r_2 = t_2 = 0.25$; (D) $r_1 = t_1 = 0.2$, $r_2 = t_2 = 0.3$; (E) $r_1 = t_1 = 0.25$, $r_2 = t_2 = 0.35$.

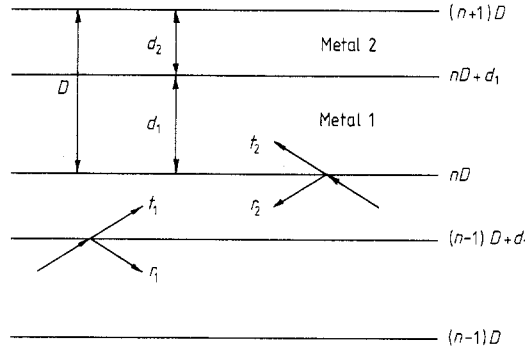


Figure 5. Illustration of metallic multiple-layer thin film.

imental and theoretical work has been done in many categories [16, 17]. For a general metallic superlattice thin film, as shown in figure 5, we make the following assumptions. First, the total number of individual layers is large enough to make the uppermost surface and the film-substrate interface effects negligible. This is a condition that can be easily fulfilled in experimental situations. Then we define t_1 , t_2 , r_1 and r_2 in the same way as we did for the double-layer thin films. The bulk material properties such as electrical conductivities, Hall coefficients, electron mean free paths, etc, are also assumed to be known. Finally, the film is in x - y plane and its dimensions in those two directions can be considered infinite in comparison with its thickness, and the magnetic field B is in the z direction. The derivation is very similar to the double-layer case, so we can eliminate some detail in the process.

Following equations (1)–(9), the electron distribution functions for multiple-layer thin films are

$$g_1^+(v, z) = \frac{eE^* \tau_1^*}{mv} \left[1 + F_1^+(v) \exp\left(-\frac{z - (n-1)D}{\tau_1^* v_z}\right) \right] \tag{36}$$

$$v_z > 0, (n-1)D < z < (n-1)D + d_1$$

$$g_1^-(v, z) = \frac{eE^* \tau_1^*}{mv} \left[1 + F_1^-(v) \exp\left(-\frac{z - (n-1)D - d_1}{\tau_1^* v_z}\right) \right] \tag{37}$$

$$v_z < 0, (n-1)D < z < (n-1)D + d_1$$

$$g_2^+(v, z) = \frac{eE^* \tau_2^*}{mv} \left[1 + F_2^+(v) \exp\left(-\frac{z - (n-1)D - d_1}{\tau_2^* v_z}\right) \right] \tag{38}$$

$$v_z > 0, (n-1)D + d_1 < z < nD$$

$$g_2^-(v, z) = \frac{eE^* \tau_2^*}{mv} \left[1 + F_2^-(v) \exp\left(-\frac{z - nD}{\tau_2^* v_z}\right) \right] \tag{39}$$

$$v_z < 0, (n-1)D + d_1 < z < nD.$$

The boundary conditions are

$$g_1^+[v_z, z = (n-1)D] = r_1 g_1^-[-v_z, z = (n-1)D] + t_2 g_2^+[v_z, z = (n-1)D] \tag{40}$$

$$g_1^-[v_z, z = (n-1)D + d_1] = r_1 g_1^+[-v_z, z = (n-1)D + d_1] + t_2 g_2^-[v_z, z = (n-1)D + d_1] \tag{41}$$

$$g_2^+[v_z, z = (n-1)D + d_2] = r_2 g_2^-[-v_z, z = (n-1)D + d_1] + t_1 g_1^+[v_z, z = (n-1)D + d_1] \tag{42}$$

$$g_2^-[v_z, z = nD] = r_2 g_2^+[-v_z, z = nD] + t_1 g_1^-[v_z, z = nD]. \tag{43}$$

Substituting (36)–(39) into (40)–(43) we obtain another set of four linear equations. For the same reason as for the double-layer thin films, we only present solutions of F in the simplified situation: interface parameters are small. The complete solutions are given in the Appendix.

$$F_1^+ = F_1^- = -1 + r_1 + t_2(\tau_2/\tau_1) - r_1 \exp[-(d_1/\tau_1^* v_z)] - t_2(\tau_2/\tau_1) \exp[-(d_2/\tau_2^* v_z)] \tag{44}$$

$$F_2^+ = F_2^- = -1 + r_2 + t_1(\tau_1/\tau_2) - r_2 \exp[-(d_2/\tau_2^* v_z)] - t_1(\tau_1/\tau_2) \exp[-(d_1/\tau_1^* v_z)]. \tag{45}$$

3.2. Conductivity and the Hall coefficient

Following equations (24)–(27), we have current densities

$$J_1^* = -\frac{4\pi e^2 m^2}{h^3} E^* \int_0^\infty dv \int_1^\infty dt v^3 \frac{\partial f_0}{\partial v} \tau_1^* (1/t^2 - 1/t^4) \times \left[1 + F_1^+ \exp\left(-\frac{z - (n-1)D}{\tau_1^* v} t\right) / 2 + F_1^- \exp\left(-\frac{z - (n-1)D - d_1}{\tau_1^* v} t\right) / 2 \right] \tag{46}$$

$$J_2^* = -\frac{4\pi e^2 m^2}{h^3} E^* \int_0^\infty dv \int_1^\infty dt v^3 \frac{\partial f_0}{\partial v} \tau_2^* (1/t^2 - 1/t^4)$$

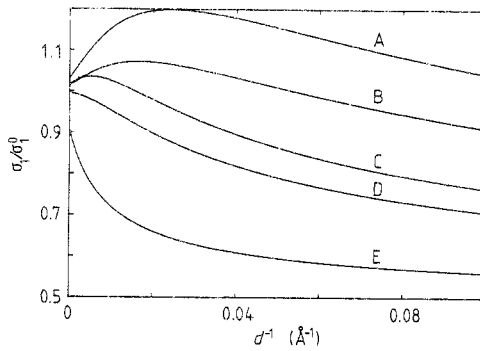


Figure 6. σ_1/σ_1^0 versus layer thickness. From top to bottom: (A) $\lambda_1 = 50 \text{ \AA}$, $\lambda_2 = 400 \text{ \AA}$, $r_1 = t_1 = 0.2$, $r_2 = t_2 = 0.3$; (B) $\lambda_1 = 50 \text{ \AA}$, $\lambda_2 = 400 \text{ \AA}$, $r_1 = t_1 = 0.1$, $r_2 = t_2 = 0.2$; (C) $\lambda_1 = 100 \text{ \AA}$, $\lambda_2 = 400 \text{ \AA}$, $r_1 = t_1 = 0.2$, $r_2 = t_2 = 0.3$; (D) $\lambda_1 = 100 \text{ \AA}$, $\lambda_2 = 400 \text{ \AA}$, $r_1 = t_1 = 0.1$, $r_2 = t_2 = 0.2$; (E) σ_2/σ_2^0 versus layer thickness, $\lambda_1 = 50 \text{ \AA}$, $\lambda_2 = 400 \text{ \AA}$, $r_1 = t_1 = 0.2$, $r_2 = t_2 = 0.3$.

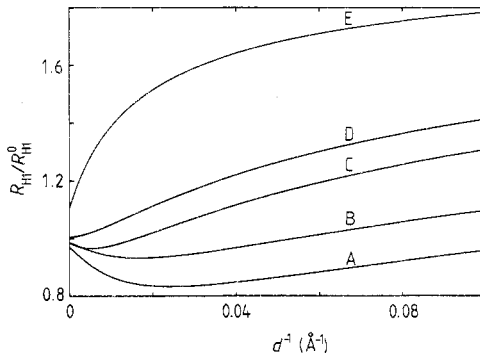


Figure 7. R_{H1}/R_{H1}^0 versus layer thickness. (A) $\lambda_1 = 100 \text{ \AA}$, $\lambda_2 = 400 \text{ \AA}$, $r_1 = t_1 = 0.1$, $r_2 = t_2 = 0.2$; (B) $\lambda_1 = 100 \text{ \AA}$, $\lambda_2 = 400 \text{ \AA}$, $r_1 = t_1 = 0.2$, $r_2 = t_2 = 0.3$; (C) $\lambda_1 = 50 \text{ \AA}$, $\lambda_2 = 400 \text{ \AA}$, $r_1 = t_1 = 0.1$, $r_2 = t_2 = 0.2$; (D) $\lambda_1 = 50 \text{ \AA}$, $\lambda_2 = 400 \text{ \AA}$, $r_1 = t_1 = 0.2$, $r_2 = t_2 = 0.3$; (E) R_{H2}/R_{H2}^0 versus layer thickness, $\lambda_1 = 50 \text{ \AA}$, $\lambda_2 = 400 \text{ \AA}$, $r_1 = t_1 = 0.2$, $r_2 = t_2 = 0.3$.

$$\begin{aligned} & \times \left[1 + F_2^+ \exp\left(-\frac{z - (n-1)D - d_1}{\tau_2^* v} t\right) \right] / 2 \\ & + F_2^- \exp\left(-\frac{z - nD}{\tau_2^* v} t\right) / 2 \end{aligned} \quad (47)$$

The expressions for electrical conductivities and Hall coefficients are the same as for double-layer films, i.e., (32)–(35). Numerical calculations of conductivity are shown in figure 6. Hall coefficient calculations are shown in figure 7. The assumed multiple-layer film consists of metal layers of equal thickness. The results are plotted against the reciprocal of the layer thickness to accommodate some experimental work [17]. In both figures curves A–D are for metal 1, and curve E is for metal 2. Again we notice that when the layers become very thick, both the conductivity and the Hall coefficient approach bulk values. The interesting feature is that under certain conditions, the conductivity and Hall coefficient for one metal have peak values. The position of the peak is quite sensitive to changes in structural parameters, as can be seen from curves

A, B and C in figure 6. Finally, curve D shows only the normal thin film size effect [2, 8]. We only plotted one curve for metal 2 due to the fact that its variation, under the assumed conditions, is relatively small in terms of structural parameters, contrary to that of metal 1. While metal 1 experiences considerable changes, metal 2 under the calculation conditions demonstrates the normal thin film behaviour [2, 8].

The appearance of peak values for metal 1 is apparently introduced by the enhanced coupling between the two metals. Unfortunately it is very difficult to predict theoretically the exact positions of the peaks, mainly due to the complexity of equations (32)–(35). However, from the results we can offer some possible explanations. First we notice that λ_1 is smaller than λ_2 , which means that the interface coupling (i.e., electron scattering) causes metal 1 to have part of its conduction electrons to hold longer mean free path λ_2 . Consequently the conductivity increases. But the total number of such electrons should be independent of the layer thickness since it is only the function of interface structure parameters and the size of the interface area. Therefore the ratio of electrons which hold λ_2 to the normal ones gets smaller when the layer becomes thicker, resulting in a lower contribution to conductivity. On the other hand, when the layer is too thin, most of the mean free paths of both types of electrons are seriously restricted by the geometry, causing the conductivity to decrease. Combining the two effects, we would expect a peak conductivity value at a certain layer thickness. From the discussion we can also see why metal 2 does not have peaks under the same assumed parameters. The second effect is that if we have better interface structure (larger values of r and t), the portion of electrons holding λ_2 within metal 1 will increase, resulting in stronger peak conductivity values. The same explanation can also be applied to the Hall coefficient.

4. Conclusions

We have presented solutions of the conduction electron distribution functions for double- and multiple-layer metallic thin films in the presence of a transverse magnetic field. From there we have derived the electrical conductivities and Hall coefficients. The results may give us some directional guidance in applying different combinations of metals and in controlling the structure of the system to achieve certain types of artificial material. The study of galvanomagnetic transport phenomena of those thin films will offer, in addition to other transport properties, another physical aspect of metal–metal interfaces. Further investigations, especially experimental ones, are very much needed for this particular problem.

Appendix

The solutions of (12)–(15) are

$$F_1^+ = -1 + p_1 + p_1 F_1^- \exp(-d_1/\tau_1^* v_z) \quad (\text{A1})$$

$$\begin{aligned} F_1^- = G^{-1} \{ & -1 + r_1 + t_2(\tau_2^*/\tau_1^*) + r_2 p_2 - t_2 p_2 (\tau_2^*/\tau_1^*) - r_1 r_2 p_2 + t_1 t_2 p_2 \\ & - (r_1 - r_1 p_1 + t_1 t_2 p_2 - t_1 p_1 t_2 p_2) \exp(-d_1/\tau_1^* v_z) \\ & - [t_2(\tau_2^*/\tau_1^*) - t_2 p_2 (\tau_2^*/\tau_1^*) - r_2 t_2 p_2^2 (\tau_2^*/\tau_1^*) + r_2 t_2 p_2 (\tau_2^*/\tau_1^*)] \\ & \times \exp(-d_2/\tau_2^* v_z) - [r_2 t_2 p_2^2 (\tau_2^*/\tau_1^*) - r_2 t_2 p_2 (\tau_2^*/\tau_1^*)] \} \end{aligned}$$

$$\times \exp(d_2/\tau_2^* v_z) - (-r_1 r_2 p_2 + r_1 p_1 r_2 p_2) \exp(d_1/\tau_1^* v_z) \} \tag{A2}$$

$$\begin{aligned} F_2^+ = G^{-1} \{ & -1 + r_2 + t_1(\tau_1^*/\tau_2^*) + r_1 p_1 - t_1 p_1(\tau_1^*/\tau_2^*) - r_1 p_1 r_2 + t_1 p_1 t_2 \\ & - (r_2 - r_2 p_2 + r_1 p_1 r_2 p_2 - r_1 p_1 r_2) \exp(-d_2/\tau_2^* v_z) \\ & - [t_1(\tau_1^*/\tau_2^*) - t_1 p_1(\tau_1^*/\tau_2^*) - r_1 t_1 p_1(\tau_1^*/\tau_2^*) + r_1 t_1 p_1^2(\tau_1^*/\tau_2^*)] \\ & \times \exp(-d_1/\tau_1^* v_z) - (t_1 p_1 t_2 - t_1 p_1 t_2 p_2) \exp(d_2/\tau_2^* v_z) \\ & - [r_1 t_1 p_1(\tau_1^*/\tau_2^*) - r_1 t_1 p_1^2(\tau_1^*/\tau_2^*)] \exp(d_1/\tau_1^* v_z) \} \end{aligned} \tag{A3}$$

$$F_2^- = -1 + p_2 + p_2 F_2^+ \exp(d_2/\tau_2^* v_z) \tag{A4}$$

where

$$G = 1 - r_1 p_1 - r_2 p_2 + r_1 p_1 r_2 p_2 - t_1 p_1 t_2 p_2. \tag{A5}$$

The complete solutions for (36)–(39) are

$$\begin{aligned} F_1^+ = G^{-1} \{ & r_1 + t_2(\tau_2^*/\tau_1^*) - 1 + [r_1^2 + r_1 r_2(\tau_2^*/\tau_1^*) - r_1] \exp[-(d_1/\tau_1^* v_z)] \\ & + [-t_1 t_2^2(\tau_2^*/\tau_1^*) + t_1 t_2 + r_1 r_2 t_2(\tau_2^*/\tau_1^*) - r_1 t_2(\tau_2^*/\tau_1^*)] \\ & \times \exp[-(d_1/\tau_1^* v_z)] \exp[-(d_2/\tau_2^* v_z)] + [-r_1^2 r_2^2 + 2r_1 t_1 r_2 t_2 + r_1 r_2^2 \\ & - t_1 r_2 t_2 - t_1^2 t_2^2 - r_1 r_2 t_2(\tau_2^*/\tau_1^*) + t_1 t_2^2(\tau_2^*/\tau_1^*)] \exp[-(d_1/\tau_1^* v_z)] \\ & \times \exp[-(2d_2/\tau_2^* v_z)] + [-r_1 r_2^2 + r_2^2 + t_1 r_2 t_2 - r_2 t_2(\tau_2^*/\tau_1^*)] \\ & \times \exp[-(2d_2/\tau_2^* v_z)] + [r_2 t_2(\tau_2^*/\tau_1^*) + t_1 t_2 - t_2(\tau_2^*/\tau_1^*)] \\ & \times \exp[-(d_2/\tau_2^* v_z)] \} \end{aligned} \tag{A6}$$

$$\begin{aligned} F_1^- = G^{-1} \{ & r_1 + t_2(\tau_2^*/\tau_1^*) - 1 + [r_1^2 + r_1 t_2(\tau_2^*/\tau_1^*) - r_1] \exp[-(d_1/\tau_1^* v_z)] \\ & + [t_1 t_2^2(\tau_2^*/\tau_1^*) + t_1 t_2 + r_1 r_2 t_2(\tau_2^*/\tau_1^*) - r_1 t_2(\tau_2^*/\tau_1^*)] \\ & \times \exp[-(d_1/\tau_1^* v_z)] \exp[-(d_2/\tau_2^* v_z)] \\ & + [-r_1^2 r_2^2 - 2r_1 r_2^2 t_2(\tau_2^*/\tau_1^*) + 2t_1 r_2 t_2^2(\tau_2^*/\tau_1^*) + r_1 r_2^2 - t_1 r_2 t_2 + t_1^2 t_2^2 \\ & + r_1 r_2 t_2(\tau_2^*/\tau_1^*) - t_1 t_2^2(\tau_2^*/\tau_1^*)] \exp[-(d_1/\tau_1^* v_z)] \exp[-(2d_2/\tau_2^* v_z)] \\ & + [-r_1 r_2^2 + r_2^2 + t_1 r_2 t_2 - r_2 t_2(\tau_2^*/\tau_1^*)] \exp[-(2d_2/\tau_2^* v_z)] \\ & + [r_2 t_2(\tau_2^*/\tau_1^*) + t_1 t_2 - t_2(\tau_2^*/\tau_1^*)] \exp[-(d_2/\tau_2^* v_z)] \} \end{aligned} \tag{A7}$$

$$\begin{aligned} F_2^+ = G^{-1} \{ & r_2 + t_1(\tau_1^*/\tau_2^*) - 1 + [r_1 t_1(\tau_1^*/\tau_2^*) + t_1 t_2 - t_1(\tau_1^*/\tau_2^*)] \exp[-(d_1/\tau_1^* v_z)] \\ & + [r_1 t_1 t_2 - r_1 t_1(\tau_1^*/\tau_2^*) - r_1^2 r_2 + r_1^2] \exp[-(2d_1/\tau_1^* v_z)] \\ & + [r_1 t_1 r_2(\tau_1^*/\tau_2^*) - t_1 r_2(\tau_1^*/\tau_2^*) - t_1^2 t_2(\tau_1^*/\tau_2^*) + t_1 t_2] \\ & \times \exp[-(d_1/\tau_1^* v_z)] \exp[-(d_2/\tau_2^* v_z)] + [2r_1 t_1 r_2 t_2 - t_1^2 t_2^2 \\ & - r_1 t_1 r_2(\tau_1^*/\tau_2^*) + t_1^2 t_2(\tau_1^*/\tau_2^*) - r_1^2 r_2^2 + r_1^2 r_2 - r_1 t_1 t_2] \\ & \times \exp[-(2d_1/\tau_1^* v_z)] \exp[-(d_2/\tau_2^* v_z)] + [r_2^2 + t_1 r_2(\tau_1^*/\tau_2^*) - r_2] \\ & \times \exp[-(d_2/\tau_2^* v_z)] \} \end{aligned} \tag{A8}$$

$$F_2^- = G^{-1} \{ r_2 + t_1(\tau_1^*/\tau_2^*) - 1 + [r_1 t_1(\tau_1^*/\tau_2^*) + t_1 t_2 - t_1(\tau_1^*/\tau_2^*)] \}$$

$$\begin{aligned}
 & \times \exp[-(d_1/\tau_1^* v_z)] + [r_1 t_1 t_2 - r_1 t_1 (\tau_1^*/\tau_2^*) - r_1^2 r_2 + r_1^2] \\
 & \times \exp[-(2d_1/\tau_1^* v_z)] + [r_1 t_1 r_2 (\tau_1^*/\tau_2^*) - t_1 r_2 (\tau_1^*/\tau_2^*) \\
 & - t_1^2 t_2 (\tau_1^*/\tau_2^*) + t_1 t_2] \exp[-(d_1/\tau_1^* v_z)] \exp[-(d_2/\tau_2^* v_z)] \\
 & + [-2r_1^2 t_1 r_2 (\tau_1^*/\tau_2^*) + 2r_1 t_1^2 t_2 (\tau_1^*/\tau_2^*) + t_1^2 t_2^2 + r_1 t_1 r_2 (\tau_1^*/\tau_2^*) \\
 & + t_1^2 t_2 (\tau_1^*/\tau_2^*) - r_1^2 r_2^2 + r_1^2 r_2 - r_1 t_1 t_2] \exp[-(2d_1/\tau_1^* v_z)] \\
 & \times \exp[-(d_2/\tau_2^* v_z)] + [r_2^2 + t_1 r_2 (\tau_1^*/\tau_2^*) - r_2] \\
 & \times \exp[-(d_2/\tau_2^* v_z)] \} \tag{A9}
 \end{aligned}$$

where

$$\begin{aligned}
 G = & 1 - r_1^2 \exp[-(2d_1/\tau_1^* v_z)] - r_2^2 \exp[-(2d_2/\tau_2^* v_z)] - 2t_1 t_2 \exp[-(d_1/\tau_1^* v_z)] \\
 & \times \exp[-(d_2/\tau_2^* v_z)] + r_1^2 r_2^2 \exp[-(2d_1/\tau_1^* v_z)] \\
 & \times \exp[-(2d_2/\tau_2^* v_z)] + t_1^2 t_2^2 \\
 & \times \exp[-(2d_1/\tau_1^* v_z)] \exp[-(2d_2/\tau_2^* v_z)]. \tag{A10}
 \end{aligned}$$

References

- [1] Sondheimer E H 1950 *Phys. Rev.* **80** 401
- [2] Jain G C and Verma B S 1973 *Thin Solid Films* **15** 115
- [3] Kinbara A and Veki K 1972 *Thin Solid Films* **12** 63
- [4] Golmaya D and Sacedon J L 1976 *Thin Solid Films* **35** 143
- [5] Chopra K L, Suri R and Thakoor A P 1977 *J. Appl. Phys.* **48** 538
- [6] Chaudhuri S and Pal A L 1977 *J. Appl. Phys.* **48** 3455
- [7] Cotter A A 1973 *J. Phys. C: Solid State Phys.* **6** 699
- [8] Tellier C R, Rabel M and Tosser A J 1978 *J. Phys. F: Met. Phys.* **8** 2357
- [9] Pichard C R, Tellier C R and Tosser A J 1980 *Thin Solid Films* **69** 157
- [10] Fuchs K 1938 *Proc. Cambridge Phil. Soc.* **34** 100
- [11] Sondheimer E H 1952 *Adv. Phys.* **1** 1
- [12] Bergmann G 1979 *Phys. Rev. B* **19** 3933
- [13] Lucas M S P 1971 *Thin Solid Films* **7** 435
- [14] Fischer B and Minnigerode G V 1981 *Z. Phys.* **B 42** 349
- [15] Dimmich R and Warkusz F 1983 *Thin Solid Films* **109** 103
- [16] Ruggiero S T 1985 *Superlatt. Microstruct.* **1** 441
- [17] Falco C M and Schuller I K 1985 *Synthetic Modulated Structures* ed. L L Chang and B C Giessen (New York: Academic) ch 9
- [18] Chen C-X 1986 *Appl. Phys. A* **40** 37
- [19] Gurvitch M 1986 *Phys. Rev. B* **34** 540
- [20] Chen C-X 1987 *Appl. Phys. A* **42** 145
- [21] Yaniv Y 1978 *Phys. Rev. B* **17** 3904
- [22] Arnold G B 1982 *Phys. Rev. B* **25** 5998
- [23] Menon M and Arnold G B 1983 *Phys. Rev. B* **27** 5508
- [24] Dobrzynski L, Djafari-Rouhani B and Hardouin Duparc O 1984 *Phys. Rev. B* **29** 3138
- [25] Das M P and Natari N 1986 *Solid State Commun.* **58** 29